

**MAGNETISM
AND FERROELECTRICITY**

Study of Magnetic Properties of $(\text{Pd}_{1-x}\text{Fe}_x)_{0.95}\text{Mn}_{0.05}$ Alloy Using Polarized Muons and Neutrons

S. G. Barsov, S. I. Vorob'ev, V. P. Koptev, S. A. Kotov, S. M. Mikirtych'yants, G. V. Shcherbakov,
L. A. Aksel'rod, G. P. Gordeev, V. N. Zabenkin, and I. M. Lazebnik

*Konstantinov St. Petersburg Nuclear Physics Institute, Russian Academy of Sciences, Gatchina,
St. Petersburg, 188300 Russia*

e-mail: vsiloa@pnpi.spb.ru

Received October 11, 2006; in final form, December 3, 2006

Abstract—The $(\text{Pd}_{1-x}\text{Fe}_x)_{0.95}\text{Mn}_{0.05}$ alloy with random competing interaction was studied by measuring the muon spin relaxation in an external transverse magnetic field and in a zero magnetic field. Using the measured temperature dependence of the dynamic relaxation rate λ and the characteristics of the distribution of local static fields, the phase states of the sample under study are refined. In particular, it is shown that the ferromagnetic and spin-glass states coexist simultaneously in the sample below 25 K. Combined studies of the sample using the μ RS and neutron depolarization methods made it possible to determine the size of magnetic inhomogeneities to be 2–6 μm in the temperature range 5–240 K.

PACS numbers: 76.75.+i, 61.12.Ex, 75.20.Hr, 75.30.Et, 75.50.Lk, 75.50.Gg, 75.47.Np

DOI: 10.1134/S106378340708015X

As is known, palladium alloys with small contents of Fe and Mn atoms belong to magnetic materials whose magnetism is caused by the interaction of the magnetic impurities through the polarized Pd matrix. The existence of two impurity types in an alloy causes ferromagnetic and antiferromagnetic exchange interactions between atoms, which differ in sign. As a result of competition of these interactions, some spins are frustrated. This has an effect on the correlations of the magnetic moments of impurity atoms on both microscopic and mesoscopic length scales. Depending on the ratio of the numbers of ferro- and antiferromagnetic bonds, various magnetic mesostructures can be formed in the alloy. For example, in $(\text{Pd}_{1-x}\text{Fe}_x)_{0.95}\text{Mn}_{0.05}$ with $x = 0.016$, as temperature decreases, ferromagnetic bonds initially play an important role and the alloy undergoes a paramagnetic-to-ferromagnetic phase transition at a temperature $T_c = 41$ K. At low temperatures, the sample transfers to the spin-glass state at $T_g = 7$ –10 K. However, polarized-neutron studies [1] detected a significant collinear magnetization component in this state, which indicates asperomagnetism at the microscopic level. The magnetic mesostructure was studied using three-dimensional neutron polarization analysis. In this method, a monochromatic neutron beam with an initial polarization vector \mathbf{P}_0 is incident on the sample. After the neutron beam passes through the sample, its polarization becomes $\mathbf{P} = \hat{D} \cdot \mathbf{P}_0$, where \hat{D} is the matrix describing the change in the polarization vector. Determining the matrix \hat{D} experimentally, one can calculate the angle φ of rotation of the polarization vector around

the direction of the average magnetization $\langle M \rangle$ and the neutron depolarization ΔP , where $\varphi \sim \langle M \rangle$ and $\Delta P = -\ln(|\hat{D}|)$.

In [1, 2], an unusual nonmonotonic temperature dependence of the neutron depolarization was detected upon cooling of a $(\text{Pd}_{1-x}\text{Fe}_x)_{0.95}\text{Mn}_{0.05}$ ($x = 0.016$) alloy sample in various magnetic fields. Figure 1 shows the temperature dependences of the rotation angle φ (Fig. 1a) and the depolarization ΔP (Fig. 1b). In low magnetic fields ($H < 5$ Oe), the depolarization increases monotonically with cooling. In such low fields, the depolarization also increases with H , whereas in fields $H > 5$ Oe the temperature dependence of the depolarization has a maximum at $T = 35$ K and the depolarization decreases as the field H increases. We note that the behavior of the average magnetization and angle φ under zero field cooling (ZFC) conditions is also nonmonotonic; at $T = 35$ K, the temperature dependence of the magnetization has a maximum. Such behavior of the magnetization is characteristic of both the collinear ferromagnet and asperomagnet, which undergo a phase transition to a state similar to the spin-glass phase.

The neutron depolarization ΔP is caused by magnetic inhomogeneities and depends on their characteristics: $\Delta P \sim (M_{\text{inh}})^2 \delta$, where M_{inh} is the remanent magnetization and δ is the average size of a domain (or a cluster). Since only the product of these characteristics enters the expressions for the depolarization, it is impossible to separate the contributions of each of them using only the depolarization data without involving theoretical models or data obtained by other experi-

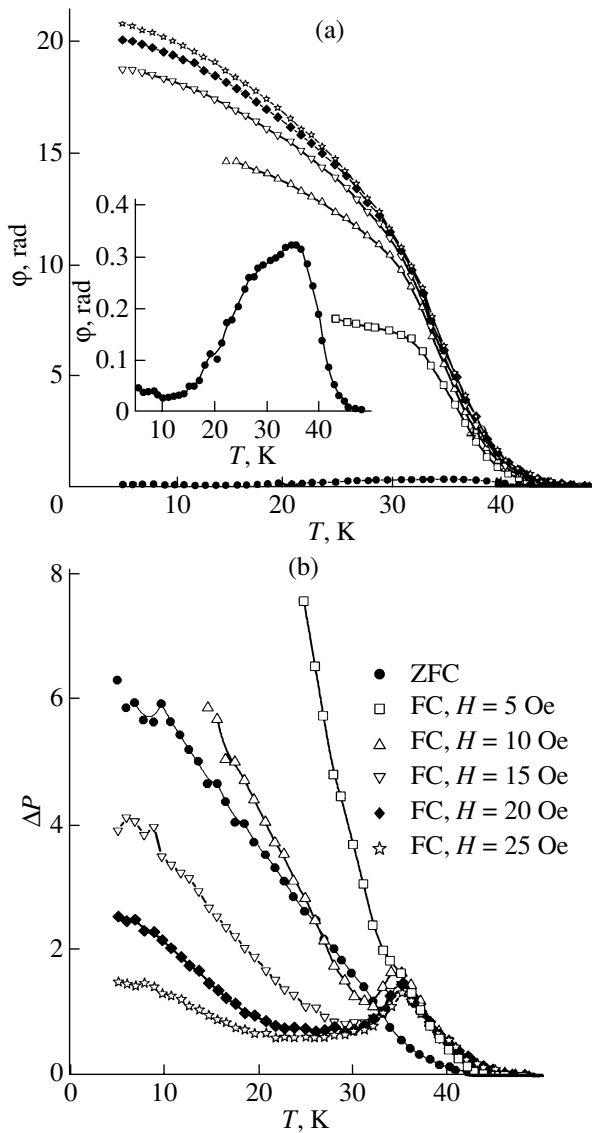


Fig. 1. Temperature dependences of (a) the rotation angle φ and (b) depolarization ΔP .

mental methods. To solve this problem, muons sensitive to local magnetization (i.e., inhomogeneity magnetization) were used.

The next stage was a μSR study of the sample at a muon channel of the synchrocyclotron at the Konstantinov Nuclear Physics Institute [3, 4]. The measurements were performed both in a zero external magnetic field and in various transverse magnetic fields over the temperature range 10–300 K.

We experimentally measured the time distributions $N_e(t)$ of positrons produced in the decay of μ^+ mesons ($\mu^+ \rightarrow e^+ + \nu_e + \tilde{\nu}_\mu$) and emitted in the direction of the initial muon polarization in the time window $\Delta t \sim 4.5\tau_\mu$ after the instant at which each muon stopped in the

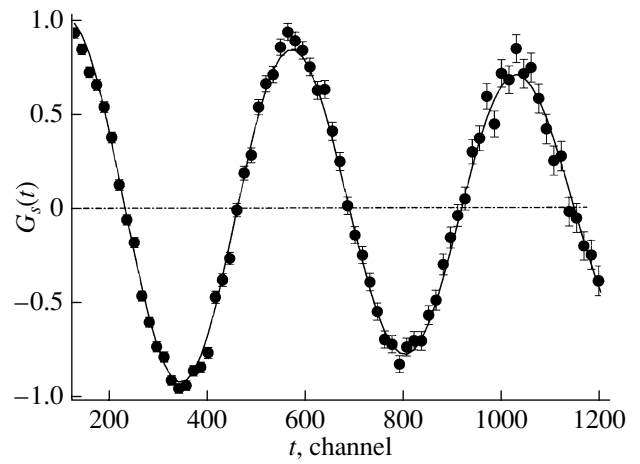


Fig. 2. Muon spin precession in an external magnetic field $H_{\perp\text{ext}} = 32.7$ Oe at $T = 61$ K; $a_{\text{tot}} = a_s + a_f = 0.2893(32)$; $\lambda = 0.077(5) \mu\text{s}^{-1}$. On the horizontal axis, one channel corresponds to 5 ns.

sample (τ_μ is the muon lifetime). The time distribution of positrons is described by

$$N_e(t) = [N_0 \exp(-t/\tau_\mu)] [1 + a_s G_s(t) + a_f G_f(t)] + \Phi, \quad (1)$$

where N_0 is the normalization factor (the number of detected positrons); $\tau_\mu \approx 2.19711 \times 10^{-6}$ s; a_s is the initial asymmetry of the decay of muons stopped in the sample and a_f is its background component from the muons stopped in the cryostat input windows in the setting counter of the muon detector; $G_s(t)$ and $G_f(t)$ are the polarization relaxation functions for muons stopped in the sample and background sources; and Φ is the background of accidental coincidences (events not correlated in time with the “start”, contributing to the distribution $N_e(t)$, where the start corresponds to the moment at which a muon stopped), which is the sum of two components, namely, the isotropic background caused by the emission of positrons produced by the decay of muons stopped in the collimator (which is intended for bounding the spatial beam size in the region of the sample under study) and the positron background caused by the temporal structure of the synchrocyclotron beam. For this sample, the accidental coincidence background is $\approx 0.6\%$ and is further taken into account in the processing of the experimental data.

In the paramagnetic region ($T > T_c > T_g$), the relaxation functions $G_s(t)$ and $G_f(t)$ have the same time dependence. Therefore, by applying an external magnetic field transverse to the muon spin to the sample (in the case under consideration, the direction of the muon spin coincides with that of the muon momentum) and processing the spectrum $N_e(t)$, we obtain the total initial asymmetry $a_{\text{tot}} = a_s + a_f$ (Fig. 2). Measurements in an external transverse magnetic field at a sample temperature below the temperature of the transition to the mag-

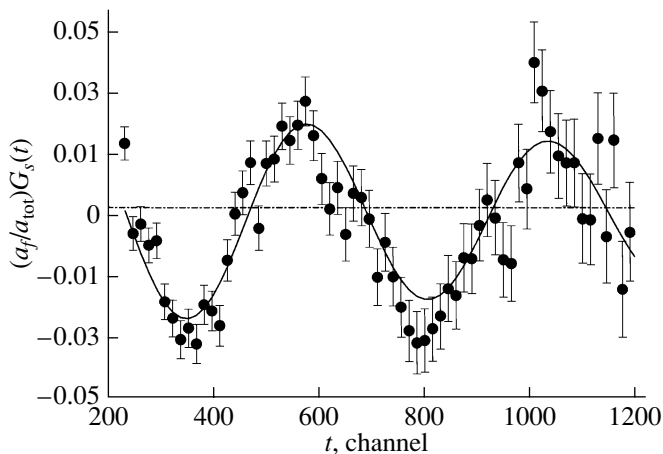


Fig. 3. Muon spin precession in an external magnetic field $H_{\text{ext}} = 32.6$ Oe at $T = 35$ K; $a_{\text{tot}} = 0.2893(32)$, $a_f = 0.0090(8)$, and $\lambda_f = 0.092(4) \mu\text{s}^{-1}$. On the time axis t , one channel corresponds to 5 ns.

netically ordered state allow one to determine the parameter a_f . In this case, in order to determine the parameter a_f , the start of the processing of the spectrum $N_e(t)$ should be shifted to larger times (by ~ 350 ns), where the contribution from the spin precession of muons stopped in the sample becomes fairly small due to rather fast relaxation caused by the relatively strong internal magnetic fields. Under these experimental conditions, the parameter a_f is $\approx 3\%$ (Fig. 3). We note that the parameters N_0 and a_{tot} depend only on the solid angle, the positron detection efficiency, and the initial muon polarization P_0 [5]. The muon spin relaxation function $G_s(t)$ as determined from $N_e(t)$ reflects the effect of local magnetic fields exerted on the muon spin in the region where the muon stopped. Within this or that model, a certain form of the function $G_s(t)$ is calculated or assumed for certain experimental conditions, after which the validity of the proposed model is verified by fitting an experimental histogram to expression (1) using the least squares method. Experimental data are analyzed assuming that the relaxation function is factorized:

$$G_s(t) = G_d(t)G_{\text{st}}(t), \quad (2)$$

where $G_d(t)$ is the relaxation function caused by dynamic effects and $G_{\text{st}}(t)$ is the relaxation function in static fields. When studying the dynamic phenomena associated with the muon spin relaxation, the relaxation function is taken in the form

$$G_d(t) = \exp(-\lambda t), \quad (3)$$

where λ is the dynamic relaxation rate. The behavior of the relaxation parameter λ allows determination of the phase transition point, since a sharp increase in λ is observed near this point due to critical fluctuations. Figure 4 shows the temperature dependence of the dynamic relaxation rate $\lambda(T)$; we can see a pronounced

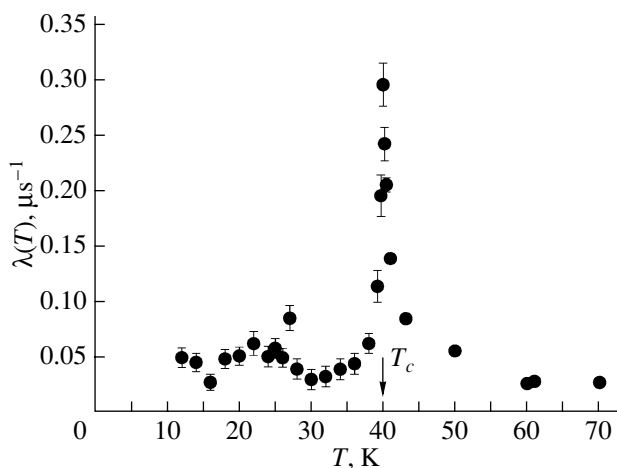


Fig. 4. Temperature dependence of the dynamic relaxation rate λ .

peak in λ at $T_c = 39.5$ K, which suggests that critical fluctuations develop near this temperature.

A further analysis of the experimental data showed that, below $T_c = 39.5$ K, the description of $G_s(t)$ will have the best value of χ^2 in the collinear-ferromagnet (CFM) model (Fig. 5)

$$G_s(t) = [1/3 + 2/3(\cos(\Omega t)\exp(-\Delta t))] \exp(-\lambda t). \quad (4)$$

The distribution function of local static fields is a Lorentzian with the average magnetic field H and the magnetic field variance Δ (Fig. 6); the temperature dependence at $T > 25$ K can be described by the relation $H \sim H_{\text{max}}(1 - T/T_c)^\beta$, where $\beta \approx 0.40 \pm 0.02$, which corresponds to the model of the Heisenberg-type 3d magnet.

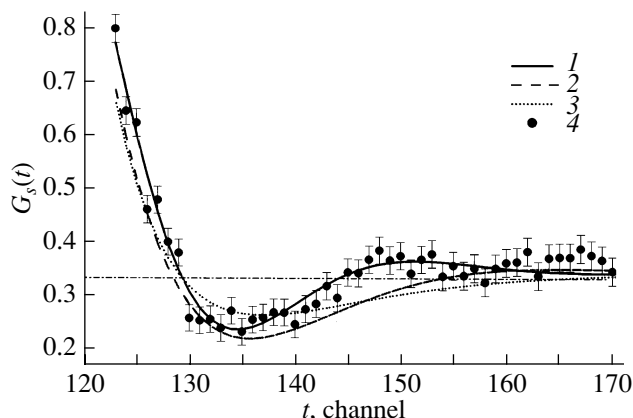


Fig. 5. Muon spin relaxation function: (1) processing within the CFM model with $\chi^2 = 1.02$, (2) processing within the ASM model with $\chi^2 = 2.26$, (3) processing within the SG model with $\chi^2 = 2.6$, and (4) experimental points obtained at $T = 28$ K in a field $H_{\text{ext}} = 0$. One channel on the time axis corresponds to 5 ns.

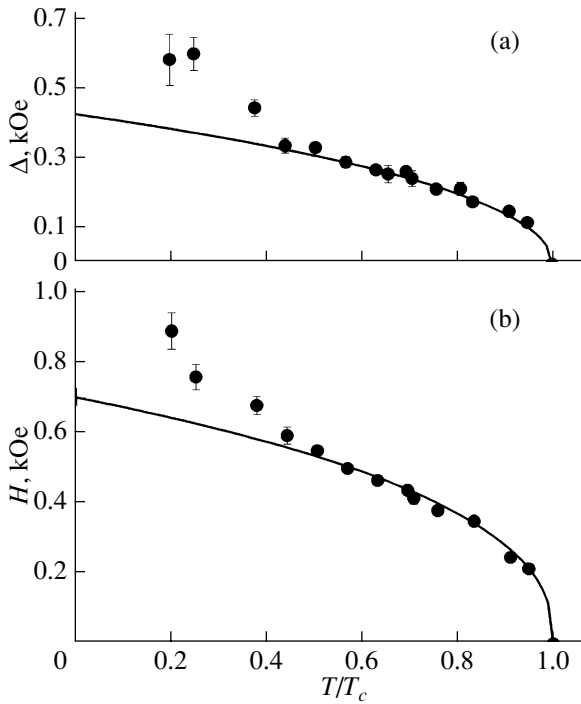


Fig. 6. Temperature dependences of (a) the variance Δ of static fields and (b) the average field H . The curves are fitting of the experimental data using the relation $H \sim H_{\max}(1 - T/T_c)^\beta$, where $\beta = 0.40 \pm 0.02$, which corresponds to the model of a Heisenberg-type $3d$ magnet.

As the temperature decreases further (below 25 K), the parameter χ^2 changes and the confidence level decreases to zero. The experimental data in Fig. 6 significantly deviate from the fitting curve and are poorly described by the model based on relation (4). None of the hypotheses proposed in [3, 4] (CFM, asperomagnet (ASM), and spin glass (SG)) yields a more or less adequate description of the G_s function. The value $\chi^2 = 1$ at 97% confidence level was achieved only in the case where the experimental data are processed using the sum of two functions, CFM + SG (Fig. 7),

$$G_s(t) = \left[a_{\text{CFM}} \left(\frac{1}{3} + \frac{2}{3} \cos(H_0 t) \exp(-\Delta_{\text{CFM}} t) \right) + a_{\text{SG}} \left(\frac{1}{3} + \frac{2}{3} (1 - \Delta_{\text{SG}} t) \exp(-\Delta_{\text{SG}} t) \right) \right] \exp(-\lambda t), \quad (5)$$

where $a_{\text{CFM}} + a_{\text{SG}} = a_s$ is the initial decay asymmetry.

By writing the initial decay asymmetry in the form of a sum of two terms describing different states, we can separate both contributions. Thus, we can conclude that two phase states coexist simultaneously in the sample below 25 K; one of these states is ferromagnetic and the other is the spin-glass state. This conclusion is consistent with the model presented by relation (5). Figure 8 shows the temperature dependence of the ratio of the spin-glass fraction asymmetry to the maximum asym-

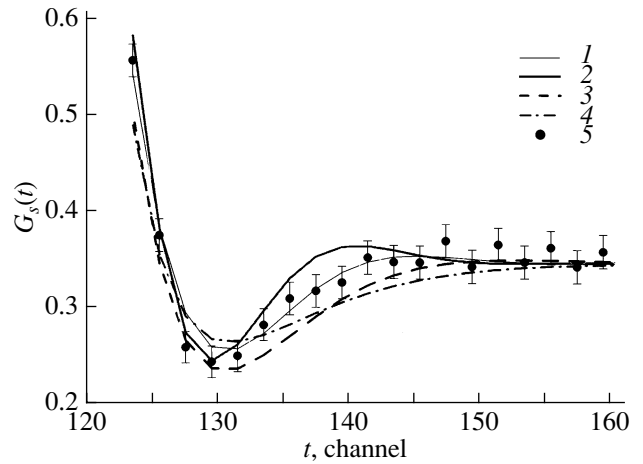


Fig. 7. Muon spin relaxation function: (1) the description by the sum of two functions CFM + SG with $\chi^2 = 1.0$, (2) processing within the CFM model with $\chi^2 = 1.23$, (3) processing within the ASM model with $\chi^2 = 1.58$, (4) processing within the SG model with $\chi^2 = 1.85$, and (5) experimental points obtained at $T = 15$ K in a zero external field. One channel on the time axis t corresponds to 5 ns.

metry. It can be seen that, as the temperature decreases, the spin-glass fraction increases long before the transition to the spin-glass state.

An analysis of the distributions of local magnetic fields shows that various magnetic states occur in the $(\text{Pd}_{0.984}\text{Fe}_{0.016})_{0.95}\text{Mn}_{0.05}$ alloy as temperature is varied (Fig. 6). For example, in the temperature range $25 < T < 39$ K, this alloy is in the CFM state with a Lorentzian distribution of local magnetic fields. In the temperature range $10 < T < 25$ K, the magnetic structure of the alloy can be considered a superposition of a collinear ferromagnet and a spin glass with a Lorentzian distribution of local magnetic fields. Below $T = 10$ K, the alloy probably undergoes a transition to the SG phase.

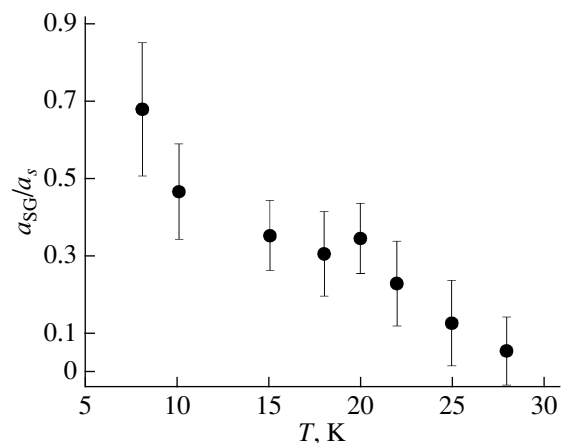


Fig. 8. Temperature dependence of the fraction of the spin-glass contribution to the depolarization of a muon ensemble.

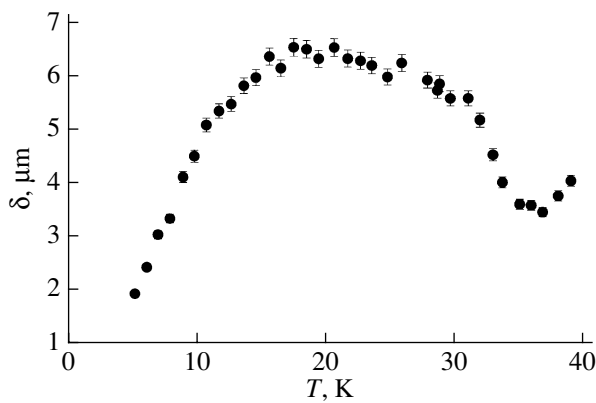


Fig. 9. Temperature dependence of the average size of magnetic inhomogeneities under cooling in a zero field.

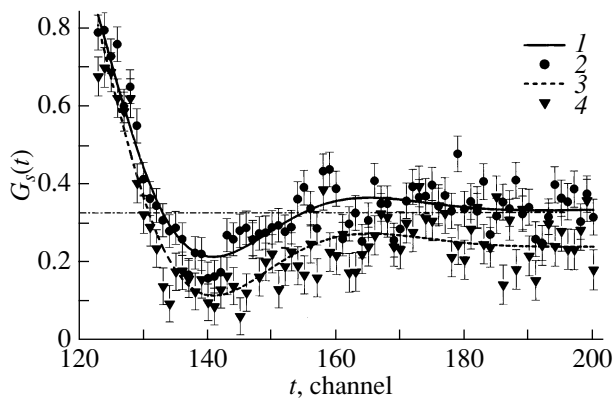


Fig. 10. Comparison of relaxation functions: (1) the description of (2) experimental points obtained in an external field $H_{\text{ext}} = 0$ at $T = 35$ K within the CFM model and (3) the description (using the function $G_s(t) = G_s(t) = a_1 e^{-\lambda t} + a_2 \cos(\Omega t) e^{-\lambda t}$, where $a_s = a_1 + a_2$) of (4) experimental points obtained in an external magnetic field $H_{\text{ext}} = 28$ Oe at $T = 35$ K. One channel on the time axis t corresponds to 5 ns.

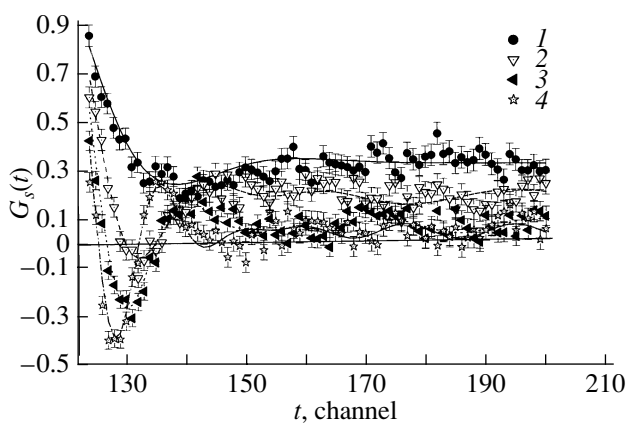


Fig. 11. Relaxation functions $G_s(t)$ for various values of the external magnetic field H_{ext} : (1) 0, (2) 410.0(2), (3) 590.0(2), and (4) 824.0(2) Oe at 35 K. One channel on the time axis t corresponds to 5 ns.

We also calculated the size δ of magnetic inhomogeneities. To estimate it, we used the data on neutron depolarization ΔP obtained upon sample cooling under the ZFC conditions (Fig. 1b). We note that the temperature dependence of the depolarization ΔP under these conditions is characteristic of samples without magnetic anisotropy (the so-called 3/2 rule is valid [6]). The quantity δ (the average size of a domain or a cluster) is calculated with allowance for the sample magnetic isotropy and assuming that the average magnetization M_{inh} of inhomogeneities is equal to the average field H (Fig. 6). The results of this calculation are shown in Fig. 9.

As seen in Fig. 10, the external transverse magnetic field penetrates the sample and magnetizes it, aligning a fraction of domains in the field direction and thereby causing a decrease in the longitudinal component of the asymmetry in the distribution of positrons. As a result, the asymptotic value of the function G_s becomes less than 1/3. This change is seen even in weak fields, 10–30 Oe (Fig. 10). For comparison, Fig. 10 shows the relaxation functions in a perpendicular magnetic field $H_{\text{ext}} = 28$ Oe and $H = 0$. In strong external fields, this change becomes even more significant and, at $H_{\text{ext}} \sim 800$ Oe, domains become completely aligned in the direction of the applied field (Fig. 11). The experimental data can be explained under the assumption that the initial asymmetry consists of three components, namely, the background (a_f), longitudinal (a_1), and transverse (a_2) asymmetries:

$$G_s(t) = a_f \exp(-\lambda_f t) + a_1 \exp(-\lambda t) + a_2 \cos(\Omega t) \exp(-\lambda t) \exp(-\Delta t), \quad (6)$$

where $a_f + a_1 + a_2 = a_{\text{tot}}$ is the total initial asymmetry of the decay.

The contribution of the transverse component increases with the external field. This results in a decrease in the asymptotic value of the function $G_s(t)$ because the external field is sufficiently high for a fraction of domains to be aligned with the applied field. Figure 12 shows the magnetic-field dependence of the degree of anisotropy, which is the ratio of the persisted initial longitudinal asymmetry to the total sample asymmetry. It is interesting that the degree of anisotropy at $T = 25$ K increases in fields of 15–30 Oe. It is not improbable that this increase can be caused by the existence of the maximum observed in the temperature dependence of the neutron depolarization in fields $H > 5$ Oe at $T = 35$ K (Fig. 1b). This phenomenon requires experimental verification and will be the subject of further study of the $(\text{Pd}_{0.984}\text{Fe}_{0.016})_{0.95}\text{Mn}_{0.05}$ sample.

This μSR study of the $(\text{Pd}_{1-x}\text{Fe}_x)_{0.95}\text{Mn}_{0.05}$ alloy with $x = 0.016$ has demonstrated once again the efficiency of this method for studying magnetic materials. The high homogeneity of the prepared sample was noted; this is suggested by the $\lambda(T)$ peak narrowness (≈ 2 K in width) in Fig. 4. At temperatures below 39.5 K

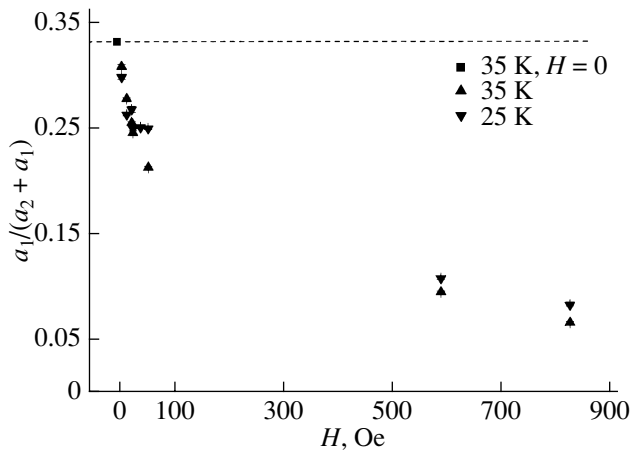


Fig. 12. Dependence of the degree of anisotropy on the external field applied to the sample.

in the zero external magnetic field, the sample is in the collinear ferromagnet state with isotropic static magnetic fields. As the temperature decreases, the spin glass fraction is formed in the sample against the collinear-ferromagnet background long before the transition to the spin-glass state, occurring presumably at $T_g = 7\text{--}10$ K. The data obtained have been used to calculate the size of magnetic inhomogeneities. The application of an external transverse magnetic field results in a gradual increase in the sample anisotropy with the applied field

and leads to the orientation of domains along the applied field.

ACKNOWLEDGMENTS

This study was supported by a program of the Division of Physical Sciences of the Russian Academy of Sciences.

REFERENCES

1. G. P. Gordeev, L. A. Axelrod, V. N. Zabenkin, I. M. Lazebnik, S. V. Grigoriev, V. Wagner, and H. Eckerlebe, *Physica B (Amsterdam)* **335**, 127 (2003).
2. G. P. Gordeev, L. A. Axelrod, S. V. Grigoriev, I. M. Lazebnik, V. N. Zabenkin, V. Wagner, and H. Eckerlebe, *Physica B (Amsterdam)* **350**, 95 (2004).
3. S. G. Barsov, A. L. Getalov, V. P. Koptev, L. A. Kuz'min, S. M. Mikirtych'yants, N. A. Tarasov, and G. V. Shcherbakov, Preprint LIYaF-1312 (Leningrad Nuclear Physics Institute, Leningrad, 1987) [in Russian].
4. V. P. Koptev and N. A. Tarasov, Preprint LIYaF-1313 (Leningrad Nuclear Physics Institute, Leningrad, 1987) [in Russian].
5. A. L. Getalov, Candidate's Dissertation (St. Petersburg Nuclear Physics Institute of the Russian Academy of Sciences, St. Petersburg, 1998) [in Russian].
6. S. V. Maleyev, *J. Phys. (Paris)* **43**, 7 (1982).

Translated by A. Kazantsev